applied sciences

MDPI

Article

Incorporation of Lignin in Bio-Based Resins for Potential Application in Fiber–Polymer Composites

Marina Machado [1], Mateus Hofmann [2], Mário Garrido [1], João R. Correia [1,*], João C. Bordado [3] and Inês C. Rosa [1]

[1] Civil Engineering Research and Innovation for Sustainability (CERIS), Instituto Superior Técnico, University of Lisbon, Av. Rovisco Pais 1, 1049-001 Lisboa, Portugal; marina.leal.santos@tecnico.ulisboa.pt (M.M.); mario.garrido@tecnico.ulisboa.pt (M.G.); ines.rosa@tecnico.ulisboa.pt (I.C.R.)
[2] Composite Construction Laboratory (CCLab), École Polytechnique Fédérale de Lausanne, CH-1015 Lausanne, Switzerland; mateus.hofmann@epfl.ch
[3] Centro de Recursos Naturais e Ambiente (CERENA), Instituto Superior Técnico, University of Lisbon, Av. Rovisco Pais 1, 1049-001 Lisboa, Portugal; jcbordado@tecnico.ulisboa.pt
* Correspondence: joao.ramoa.correia@tecnico.ulisboa.pt

Abstract: Bio-based resins, obtained from renewable raw materials, are a more sustainable alternative to oil-based resins for fiber-reinforced polymer (FRP) composites. The incorporation of lignin in those resins has the potential to enhance their performance. This paper presents results of an experimental study about the effects of Lignoboost lignin incorporation on a partially bio-based vinyl ester (VE) resin. Two resins were prepared—without (reference) and with lignin addition (4% by weight) to its main chain—and their chemical, thermophysical, and mechanical properties were compared using Fourier transform infrared (FTIR) spectroscopy, gel permeation chromatography (GPC), dynamic mechanical analysis (DMA), thermogravimetric analysis (TGA), and tensile and shear tests. Results suggest that the addition of lignin to the base resin resulted in a copolymer of increased heterogeneity and higher molecular weight, incorporating stiff and complex aromatic structures in the polymer chain. While requiring high-temperature curing, the VE–lignin copolymer presented improvements of 27% in tensile strength, 4% in shear strength, and increased glass transition temperature by about 8 °C, thus confirming the potential of this natural biopolymer for FRP composite applications.

Keywords: bio-based composites; bio-resin; Lignoboost lignin; natural polymer; fiber-reinforced polymers; thermomechanical properties; mechanical properties

Citation: Machado, M.; Hofmann, M.; Garrido, M.; Correia, J.R.; Bordado, J.C.; Rosa, I.C. Incorporation of Lignin in Bio-Based Resins for Potential Application in Fiber–Polymer Composites. *Appl. Sci.* **2023**, *13*, 8342. https://doi.org/10.3390/app13148342

Academic Editor: Guan Seng Tay

Received: 21 June 2023
Revised: 13 July 2023
Accepted: 17 July 2023
Published: 19 July 2023

1. Introduction

Over the past two decades, the use of fiber-reinforced polymer (FRP) composites has grown steadily as a response to the durability and sustainability challenges associated with traditional materials, such as reinforced concrete, steel, and timber [1,2]. In particular, FRP composites have been gaining increased importance in structural applications in various industries due to their corrosion resistance and high strength-to-weight and stiffness-to-weight ratios. Moreover, due to their lightness, their installation is typically fast, leading to increased efficiency during the construction stage [3].

The environmental sustainability of FRPs is now one of the top concerns of the composites industry, with one of the key issues being the fact that conventional polymeric resins are derived from crude oil. This concern has prompted the development of bio-based alternatives to the industry-standard oil-derived resins, which, in addition to incorporating sustainably sourced monomers (i.e., derived from renewable raw materials), also show comparable mechanical performance to their oil-based counterparts [4–7]. The byproducts of biomass refinery, such as 1,3-propanediol, isosorbide, fumaric acid, vanillin, limonene, and itaconic acid, are examples of bio-derived monomers that have recently been used to

produce biopolymers and biofuels with lower carbon footprints than their conventional counterparts [5,6].

Lignocellulosic biomass, derived from forests, is the most abundant type of biomass and a valuable source of natural polymers, such as cellulose, hemicellulose, and lignin. In turn, lignin is the second most abundant natural polymer and can be recovered as a byproduct of the pulp and paper industry [8]. Lignin is an amorphous and heterogeneous polymer with high molecular weight and takes the form of a complex three-dimensional structure of alkylphenolic rings that result from the polymerization of three types of aromatic monomers: p-coumaryl alcohol, coniferyl alcohol, and sinapyl alcohol [9,10]. These copolymerize to form the lignin structural units syringyl (S), guaiacyl (G), and p-hydroxyphenyl (H), with their proportions in the polymer depending on the biomass source (i.e., the type of vegetation) [11]. Due to its partly aromatic backbone, lignin offers good thermal stability and fire retardancy, making it suitable for applications where increased heat resistance and improved fire reaction performance is required [12]. Moreover, lignin is very stiff, owing to the strong bonds that hold the monomers together.

The incorporation of lignin in resins used in the production of FRP composites; therefore, it has excellent potential to enhance the sustainability of these materials by increasing their renewable content as well as by potentially improving their mechanical properties at ambient temperature and their high temperature resistance (due to the presence of aromatic rings with high thermal stability) and fire reaction properties. Through the biorefining of lignin, valuable aromatic structures akin to phenol can be obtained; however, the depolymerization processes required to achieve this are costly [9,13], which explains why this natural polymer has been mostly incorporated into resins, adhesives, foams, and other polymeric materials in its macromolecular form [14–19]. In fact, several efforts have been made in recent years to incorporate lignin into the polymer structures of phenolic [20–22], polyurethane [23], furanic [24], epoxy [25–27], polyester [28–30], vinyl ester [30,31], and acrylate-based [32,33] resins.

A common issue in these studies is determining the actual role of the macromolecular lignin in the resulting material. The combination of base polymer and lignin can result in (i) a composite in which the lignin acts as a filler and there is a well-defined interface with the base polymer, (ii) a blend of lignin and a base polymer wherein interdiffusion between the two polymers occurs, and (iii) a copolymerized network in which lignin acts as a reactive component, either integrating the main polymer structure or functioning as a crosslinking agent [11,27]. The actual incorporation mechanism will be dependent on several factors, including but not limited to the compatibility between the base polymer and the type of lignin used, as well as the process(es) used for lignin incorporation. Depending on the type of combination between lignin and the base polymer, the properties of the resulting material can vary significantly, with both reductions and increases in performance having been reported in previous studies [11].

Among the previously mentioned resin types, those derived from phenol are very interesting for applications where the thermal behavior is a relevant performance requirement, given their low flammability and good mechanical properties at relatively high temperatures (up to around 200 °C [34,35]). Such properties are highly desirable in FRP composites used in many applications. However, the use of phenolic resins in FRP materials is hindered by difficulties associated with the production, reinforcement, and thermal curing of these resins, in addition to their brittleness at ambient temperature and low impact resistance [36,37].

Considering this context, the greatest potential for the use of lignin in bio-based resins for FRP composites seems to lie in its incorporation in the polymer structure of the types of resin more commonly used in the composites industry, such as unsaturated polyester or vinyl ester. The present study explores this strategy by investigating the effects of lignin incorporation (4% w/w) on a partially bio-based vinyl ester resin synthesized in a two-step bulk polycondensation reaction. The bio-based resin was formulated with monomers derived from renewable sources, namely 1,3-propanediol, isosorbide, and fumaric acid,

and ortho-phthalic anhydride, sourced from crude oil. The objective of lignin incorporation was two-fold: (i) to increase the bio-based content of the vinyl ester resin and (ii) to improve the stiffness of the main polymeric chain, and thus, the mechanical properties of the resin. To that end, two bio-based vinyl ester resin compositions were produced, one without (reference formulation) and another with lignin incorporation. These resins were characterized by means of the following analyses/tests: (i) Fourier-transform infrared (FTIR) spectroscopy, (ii) gel permeation chromatography (GPC); (iii) dynamic mechanical analysis (DMA), (iv) thermogravimetric analysis (TGA), (v) tensile tests, and (vi) shear tests.

2. Materials and Methods

2.1. Materials

Two partially bio-based vinyl ester (VE) resins were produced in this study: a reference bio-based VE resin (BVE) and a bio-based VE resin incorporating lignin in its main polymeric chain (BVEL); the prepolymers of both resins presented a mass bio-based content over 80%. The base formulation of the bio-based VE resin was obtained from the modification of the polymeric chain of a bio-based unsaturated polyester resin, previously developed at Instituto Superior Técnico, which was recently used for the pultrusion of carbon fiber-reinforced polymer laminates [5]. This bio-resin was formulated with monomers obtained from renewable sources (1,3-propanediol, isosorbide, and fumaric acid) and non-renewable sources (ortho-phthalic anhydride).

The following materials were used in the synthesis of the resins: 1,3-propanediol (PDO) was acquired from *DuPont and Tate and Lyle* under the commercial name of *Susterra*^{TM} *propanediol*; isosorbide (ISO, >98%) was provided by *Tokyo Chemical Industry Co.* (*TCI*, Tokyo, Japan); fumaric acid (FA, >98%), ortho-phthalic anhydride (PA) (99%), and 2-hydroxyethyl methacrylate (HEMA, 97%) were obtained from Sigma Aldrich; styrene (STY), cobalt octoate 1% (OC), and methyl ethyl ketone peroxide (PMEK) were provided by *EcoCompósitos S.A.* (Portugal). All reagents were used without modification (i.e., as received), except for the Kraft lignin, obtained through the Lignoboost process, which was washed with distilled water prior to the synthesis to extract its inorganic phase. This lignin was extracted from Eucalyptus wood, a softwood for which the H/G/S proportions were reported to be in the range of 0–5/95–100/0 (%) [38].

2.2. Synthesis

The prepolymers were obtained through a two-step bulk polycondensation reaction (described below), following the formulations listed in Table 1 and with the chemical structure depicted in Figure 1, which illustrates how lignin is incorporated in the bio-based prepolymer. The lignin structure is linked by covalent bonds in the structure of the linear vinyl ester prepolymer. Depending on the lignin content, each vinyl ester backbone can have one or more lignin derived segments but not more than three to avoid premature reticulation.

Both BVE and BVEL resins were formulated with a mixture of unsaturated (PA) and saturated (FA) acids, at a mass ratio of 1:2.5. BVE and BVEL resins were synthesized using a glycol excess of 15% and 12% in mol, respectively (in the latter case, the glycol excess aimed to compensate for uncertainties arising from the polycondensation reaction of the lignin). In the BVEL resin, 0.1 mol % of isosorbide (regarding the total glycol amount) was replaced by 35.74 g of lignin, corresponding to a total incorporation ratio of lignin of ca. 4% *w*/*w*, (slightly) increasing the prepolymer bio-based mass content from 82.1% to 82.8%.

The reactants were placed inside a 2 l reactor equipped with a bottom drain valve, a glass lid with 5 ground joints, an anchor blade mechanical stirrer, a nitrogen gas inlet, and an addition funnel (to add the FA in the second stage of the synthesis, as described below). The reactional medium was heated at 206 °C ± 4 °C using a heating mantle, and the temperature inside the reactor was monitored with a thermocouple. The residual water formed during synthesis and the water derived from the solubilization of the raw

materials was collected using a condenser coupled to a distilling receiver (Dean–Stark type apparatus).

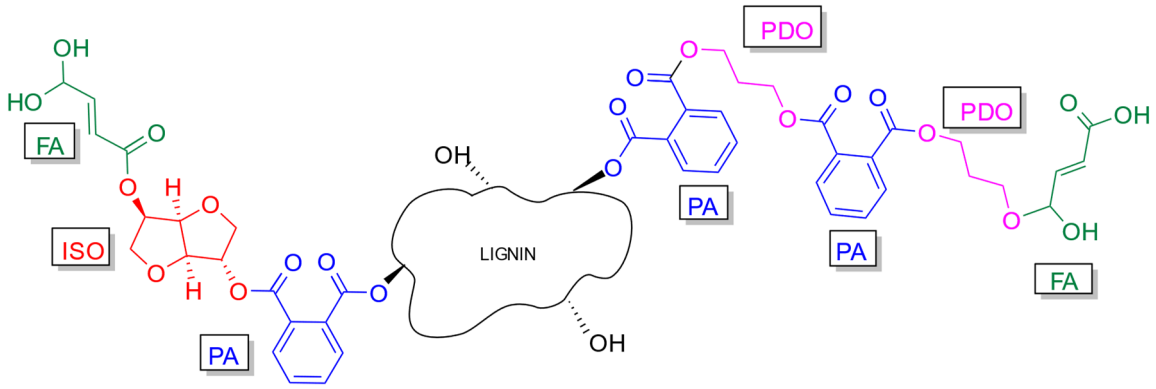

Figure 1. Chemical structure of the prepolymers used in the synthesis of resin BVEL.

Table 1. Dry mass content of BVE and BVEL resins.

Monomer	BVE Resin	BVEL Resin
	Dry Mass Content (g)	Dry Mass Content (g)
Ortho-phthalic anhydride (PA)	148.11	148.11
Fumaric acid (FA)	292.18	292.18
1,3-propanediol (PDO)	187.99	197.27
Isosorbide (ISO)	200.58	188.29
Lignin	-	35.74

In the first stage of the synthesis, the reactants were added to the reactor at ambient temperature, and then stirred and heated to the set-point temperature to promote the bonding between the OH groups of glycols and the COOH groups of PA. During this stage, the reaction progress was monitored through acid-base titration, and the reaction proceeded until the acid number (AN) stabilized below 30 mgKOH/g. In a second stage, the reactor was cooled to 100 °C and the stirring motion was slowed to incorporate the FA in the reaction medium. This two-step procedure ensured that the unsaturated double bonds of FA were formed at the extremities of the polymeric chains, making the resin less hydrophilic than an unsaturated polyester (UP) resin (as there are fewer unsaturation points in the polymeric chain), and thus enabling a vinyl ester molecular structure (with less saturation points over the polymeric chain) to be obtained. The second stage of the polycondensation reaction proceeded until the AN stabilized (same value in two consecutives measurements, one hour spaced) or until the maximum viscosity reached 16,000 cp (the viscosity was measured at 125 °C in a high-temperature ICI cone and plate viscosimeter); once one of these criteria was satisfied, the prepolymers were cooled to a temperature of 160 °C. Afterwards, they were diluted (without prior purification) in a balanced mix of STY and HEMA at an incorporation temperature between 60 °C and 70 °C. The use of reactive diluents in the processing stage allowed the adjustment of the viscosity of the final product, whereas in the hardening stage they promoted the connection between the linear chains of VE (through the crosslinking points of the unsaturated double bonds of FA), thus forming a thermosetting crosslinked structure.

Of the various formulations tested (in which the ratio between PA and FA was varied between 1.5 and 3.5), the resin compositions shown in Table 1 were the ones that presented a better balance between mechanical and thermomechanical properties and processing parameters (for different manufacturing techniques of FRP composites), and they aimed at maximizing the overall bio-based content. Indeed, these bio-based VE resins were produced with monomers predominantly derived from renewable resources, and they

also incorporated a lower styrene content (partially replaced by HEMA) compared to conventional VE resins. It is worth mentioning that styrene is more toxic than HEMA, despite the former being commonly used as the sole reactive diluent in conventional VE and UP resins; the use of HEMA therefore has fewer harmful effects on human health and on the environment [39].

2.3. Specimen Preparation

The resin plates used for specimen characterization had a thickness of 4 mm and were produced differently for BVE and BVEL resins since, due to the phenolic nature of lignin, the latter resin required curing at an elevated temperature (80 °C). This caused certain difficulties in terms of limiting the maximum size of the BVEL plates and their frequent cracking.

The resin plates were produced in open molds comprising two tempered glass plates with dimensions of 500 × 500 mm^2 for the BVE resin and 200 × 200 mm^2 for the BVEL resin (to enable curing inside a thermal chamber). The gaps between the glass plates of the BVE and BVEL resins were sealed with a rubber or silicone cord, respectively, and acrylic spacers (4 mm thickness) were placed adjacently (and externally) to the cord. A releasing agent was sprayed on the surface of the molds to ease the separation of the cured resin plate from the glass molds.

The BVE resin plates were cured for 24 h at ambient temperature (20 ± 2 °C), while those with BVEL resin were cured for 3 h at 80 °C. Afterwards, they were both post-cured at 100 °C for 4 h and then cooled to an ambient temperature. In addition, one batch of BVEL resin was post-cured at 110 °C for 24 h. All test specimens were cut according to standardized dimensions (see Section 2.4) in a CNC machine.

2.4. Characterization Tests

Fourier transform infrared (FTIR) analysis was performed on the bio-based prepolymer, without and with lignin incorporation. A *Spectrum Two Perkin Elmer* spectrometer was used, and the spectra were captured from 4000 to 600 cm^{-1} and analyzed in *Perkin Elmer Spectrum IR* software, version 10.7.2.

Gel permeation chromatography (GPC) tests were carried out in the prepolymer without and with lignin incorporation to determine their molecular weight average number (M_n) and molecular weight average weight (M_w). Tetrahydrofuran (THF) was used as the solvent, according to ISO 13885-1, at a concentration of 1 mg/mL. The samples underwent filtration and were then injected into a column set, which consisted of a precolumn (8 × 50 mm) PSS SDV and columns (8 × 300 mm) PSS SDV analytical linear S, both with a particle size of 3 µm, and filled with polystyrene crosslinked with divinylbenzene (gel). Prior to elution, the columns were equilibrated at 40 °C, and then a flowing rate of 1.0 mL/min was used. Dual detectors held at 40 °C were employed to monitor the eluent: the first was a UV/Visible detector (model JASCO UV-4075) set at 254 nm and the second was a refractive index detector (model JASCO RI-4030). The molecular weights were calculated based on the retention time using a conventional calibration method with narrow polystyrene standards (M_n ranging from 266 to 59,300 Da).

DMA tests were performed to assess the influence of the aromatic groups of lignin in the thermo-mechanical behavior and in the glass transition temperature (T_g) of the bio-based VE resin, determined according to ISO 6721-11. The experiments were conducted according to the ASTM E1640 [40] standard in a *Q800 TA Instruments* dynamic mechanical analyzer. The specimens were tested in a dual cantilever configuration, considering a deformation amplitude of 15 µm and 10 µm, respectively, in BVE and BVEL specimens, as well as an oscillatory frequency of 1 Hz. The tests were performed from −30 °C to 150 °C, at a heating rate of 2 °C/min. For each type of resin, two replicate specimens were tested and, in the case of the BVEL resin, two runs were carried out to assess the effects of exposure to elevated temperature (above the post-curing temperature) regarding the thermomechanical behavior of the material, and a third specimen was tested after post-cure

for a longer period at a higher temperature to assess the effects of the additional post-cure. Table 2 lists the specimens tested, indicating the post-curing conditions and the number of DMA runs.

Table 2. Summary of DMA experiments.

Resin	Specimen	Post-Curing		Runs
		Temperature (°C)	Time (h)	
BVE	BVE-1	100	4	1
	BVE-2			1
BVEL	BVEL-1			2
	BVEL-2			2
	BVEL-3	110	24	1

Thermogravimetric analyses (TGA) were also conducted according to ASTM E2550-21 [41] standard on a *Hitachi-STA7200* analyzer. These tests aimed at quantifying the mass variation of the resins as a function of temperature and estimating their decomposition temperatures. The experiments were conducted on two samples for each resin with mass of 15–30 mg, from ambient temperature (20 °C) up to 600 °C, at a heating rate of 10 °C/min, and in both oxidative (synthetic air) and inert (nitrogen) atmospheres (air flow of 100 mL/min).

The mechanical behavior of the resins was compared by means of tensile and shear tests conducted according to ASTM D638-14 [42] and ASTM D5379/D5379M [43] standards, respectively, and the shear tests were performed according to the V-notched beam method. For each test type, five replicate specimens of the BVE resin and three of the BVEL (due to the aforementioned difficulties in obtaining cured material for testing) were tested in an *Instron* universal testing machine (model 5982, with load capacity of 100 kN); the tests were performed under displacement control, at a displacement rate of 1 mm/min. Displacements were measured at different points of the specimens with a video extensometer, which comprised a high-resolution *SONY* camera (model XCG-5005E) with *Fujinon* lens (model *Fujifilm* HF50SA-1). This system enabled us to track the position of a set of points (targets) marked on the surface of the specimens during the tests and then compute the relative displacement (i.e., deformation) between those points to estimate the elastic and distortion moduli of the resins.

3. Results and Discussion

3.1. FTIR

The FTIR spectra of the partially bio-based prepolymers, without and with lignin incorporation, are depicted in Figure 2. As expected, due to the relatively low incorporation of lignin (4% wt.), the same band patterns were found in the FTIR spectra of both bio-based resins. The carbonyl stretching mode of the ester groups can be associated with the intense bands in the region of 1715 cm^{-1} [44], whereas the band in the region of 1250 cm^{-1} can be attributed to the C-O-C and C-O stretching of those same groups [45]. The (-C=C-) double bond from fumaric acid is apparent in the band located at 1645 cm^{-1} [46]. Regarding the transmittance peaks in the regions of 1600 cm^{-1} and 1475 cm^{-1}, these should highlight the presence of the aromatic rings in the polymer structure. The bands in the region of 2900 cm^{-1} can be attributed to the stretching vibration mode of methylene (-CH2-) [47]. The band corresponding located in the region of 3500 cm^{-1} can be attributed to the vibration of the hydroxyl group (-OH) [48].

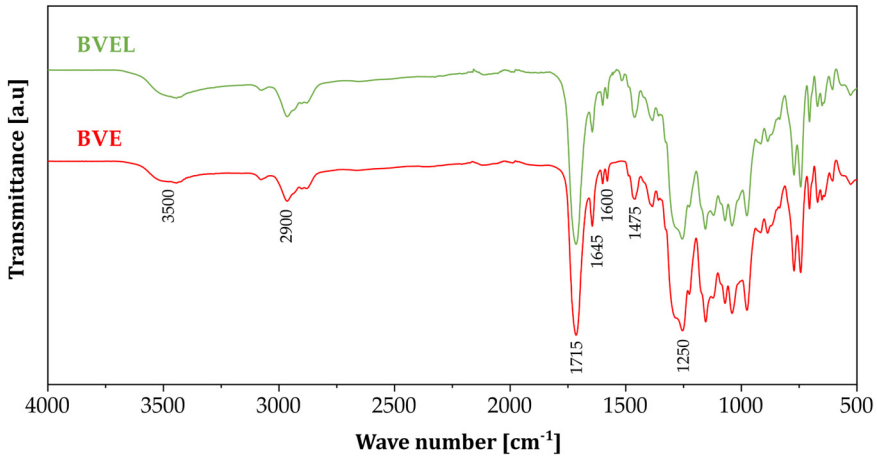

Figure 2. FTIR spectra of bio-based prepolymers, without and with lignin incorporation.

3.2. GPC

Figure 3 shows the retention time results from the GPC analyses performed on the bio-based resins without and with lignin incorporation. Table 3 summarizes the resulting values of M_n, M_w, and polydispersity index (PDI).

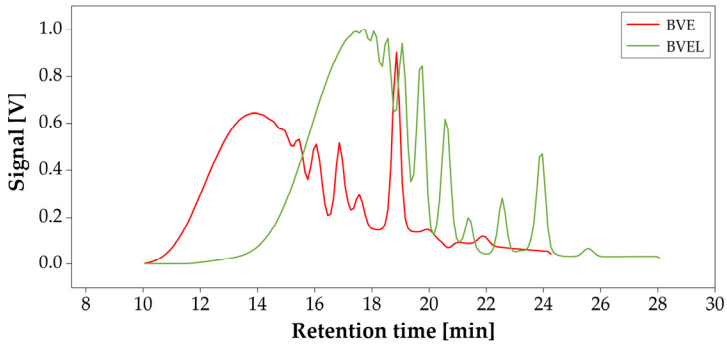

Figure 3. GPC spectra of the two bio-based prepolymers (without and with lignin incorporation).

Table 3. Summary of GPC results.

Parameter	BVE	BVEL
M_n	1555	1483
M_w	2956	3561
PDI	1.9	2.4

The differences in spectra obtained for BVE and BVEL suggest that the incorporation of lignin in the linear vinyl ester was overall successful, having produced a significant increase (20%) in the molecular weight of the lignin-containing prepolymer relative to the base prepolymer. The PDI obtained for the BVEL prepolymer was also higher (26%), indicating an increased heterogeneity of the polymer segments.

3.3. DMA

Figure 4 presents the storage modulus (E') and tangent delta (tan δ) curves obtained from DMA both as function of temperature. Table 4 presents the values of T_g obtained from each of the curves plotted in Figure 4. The thermomechanical response of the BVE and BVEL resins mostly present similar qualitative behavior, with some differences in the behavior immediately following the glass-transition process, which are discussed below (in this section). For both resins, the storage modulus showed a sigmoidal variation with

increasing temperature, which was characterized by an initial plateau during the vitreous state, followed by a steep reduction due to the softening of the resin during the glass transition process; accordingly, this process is also correlated with the peaks of the tangent delta curves. The T_g values obtained from the onset of E' decay were relatively similar for the resins cured for 4 h at 100 °C (BVE-1,2 and BVEL-1,2), being in the 55–60 °C range; the T_g estimates obtained from the tan δ peak were in the range of 95–105 °C, with the BVEL samples at the higher end of this range.

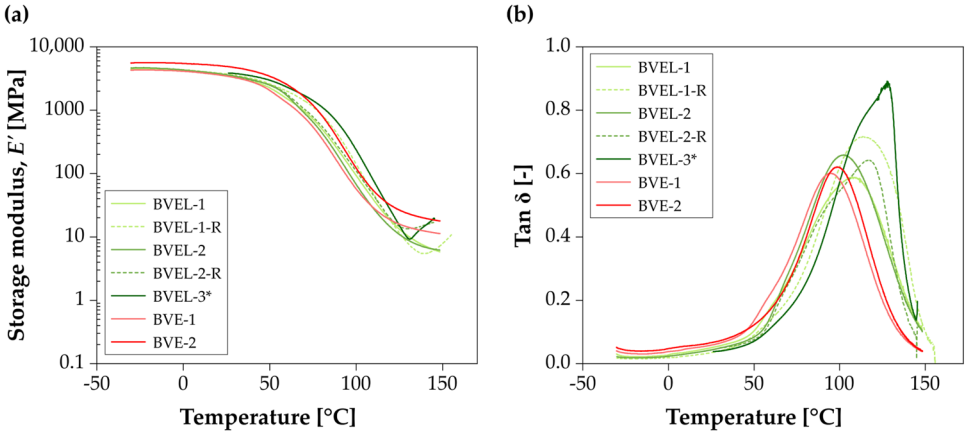

Figure 4. DMA results: (**a**) storage modulus and (**b**) tangent delta curves of BVE and BVEL resins as a function of temperature (* specimen cured for 24 h at 110 °C; remaining specimens cured for 4 h at 100 °C).

This slight performance improvement of the BVEL resin (reflected in higher T_g values) suggests that the incorporation of lignin somewhat reduced the polymer chain mobility compared to the reference resin. This was expected considering that lignin is a complex and heterogeneous natural polymer with a relatively high molecular weight and rather rigid aromatic segments and considering its effects on the molecular weight of the prepolymers as discussed for the GPC analysis. The magnitude of the tan δ peaks for the two resins was also significantly different, being 5 to 10% higher in BVEL. This further suggests a more amorphous and heterogeneous (less crystalline) polymer structure in that resin compared to BVE.

Table 4. Summary of DMA results.

Resin	Specimen	1st Run			2nd Run		
		T_g, E'	T_g, tan δ	Failure	T_g, E'	T_g, tan δ	Failure
BVE	BVE-1	54.9	94.9	No	(-)	(-)	(-)
	BVE-2	62.1	98.3	No	(-)	(-)	(-)
BVEL	BVEL-1	57.6	107.2	No	66.2	116.8	Yes
	BVEL-2	58.3	102.3	No	69.2	114.3	Yes
	BVEL-3 *	79.7	145.7	Yes	(-)	(-)	(-)

* Specimen cured for 24 h at 110 °C (remaining specimens cured for 4 h at 100 °C).

However, it is important to note that the BVEL-3 specimen, post-cured for 24 h at 110 °C, exhibited significantly higher T_g values, estimated both from the onset of E' decay (79.7 °C) and tan δ peak (145.7 °C); additionally, this specimen exhibited a sudden increase in E' following the glass transition process, failing due to bending inside the DMA chamber shortly after. The peak of tan δ occurred during this segment of the material's response, resulting in the unusual development of this curve; this should be taken into account when considering the T_g estimate taken from the tan δ peak for this specimen.

To further investigate this observation, the remaining BVEL samples were subjected to a second DMA run, during which similar post-glass-transition behavior (E' increase

followed by failure) was observed. Additionally, as expected, these samples presented increased T_g in the second run (in the range of 66–69 °C from the onset of E' decay and 114–116 °C from tan δ peak) relative to the first run, suggesting increased crosslinking from the consecutive heating processes undergone during DMA. In fact, the results gathered from the BVEL-3 specimen (significantly increased T_g after longer post-curing at higher temperature), combined with the results from the second run of the BVEL-1 and 2 specimens, indicate that there was still significant potential for additional cross-linking in the BVEL resins even after post-curing at 100 °C for 4 h. It is reasonable to consider that the increases in E' after glass-transition may have resulted from additional cross-linking being facilitated by the polymer's state of increased molecular mobility.

Similar post-glass-transition increases of E' have been reported in the literature for acrylate-based resins incorporating lignin, either as a filler or as part of a copolymerized network [33]. In that study, the authors also suggested that lignin may have contributed to further crosslinking at elevated temperatures, thus resulting in increased E'.

3.4. TGA

Figure 5 shows the percentage of remaining mass vs. temperature curves and the derivative of the mass loss curve (DTG) obtained from TGA tests in oxidative and inert (nitrogen) atmospheres. Table 5 summarizes the main results of the TGA tests, namely the temperatures for the mass reductions of 5%, 10%, and 50% (often used to define the decomposition temperature) and the mass residue (in %).

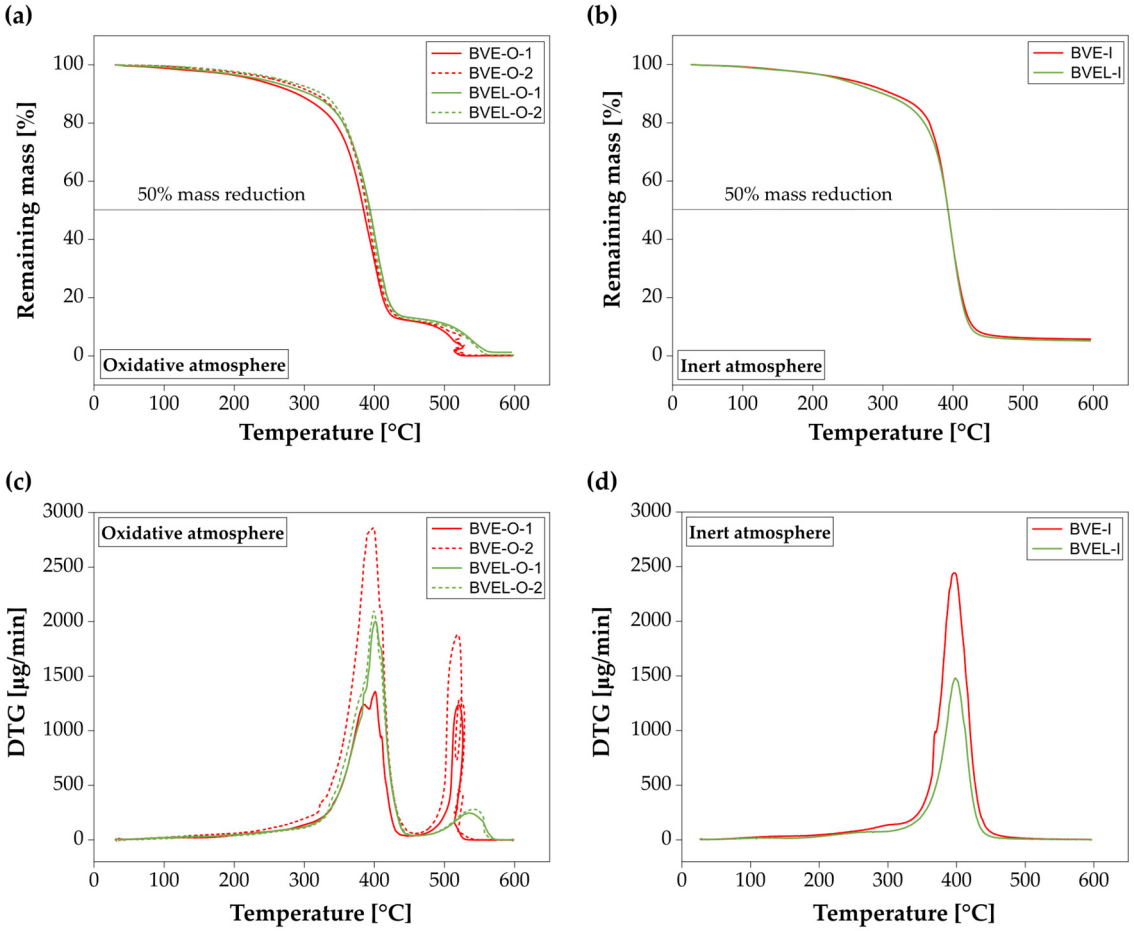

Figure 5. TGA results: the remaining mass (**a**,**b**) and the derivative of mass loss curve (DTG) (**c**,**d**) of BVE and BVEL resins as a function of temperature.

In an oxidative environment, the remaining mass of the BVE and BVEL resins showed an almost identical two-step sigmoidal variation with increasing temperature (two peaks in DTG): while mass was reduced moderately at ~300 °C, it dropped sharply between ~300 °C and ~420 °C, and then between ~500 °C and ~600 °C, due to the thermal decomposition of the resins with a slight lag (~10 °C) between the BVE and BVEL resins (the disturbance in the BVE curve at ~500 °C, which occurred for the two samples, is likely due to smoke release during combustion of the resin). In an inert environment, the remaining mass curves of the BVE and BVEL resins almost overlapped, presenting a single drop (one peak in DTG) to between ~300 °C and 420 °C.

In an oxidative atmosphere, the decomposition temperature, defined for a mass reduction of 50% with respect to that at ambient temperature, is 387 °C and 393 °C for resins BVE and BVEL, respectively. This confirms the positive impact, even if slight, of introducing the complex aromatic lignin structures into the resin's polymeric chain. For the inert atmosphere, the decomposition temperature of both resins is 393 °C.

Table 5. Summary of TGA results.

Atmosphere	Resin	Specimen	$T_{5\%}$ (°C)	$T_{10\%}$ (°C)	$T_{50\%}$ (°C)	Residue (%)
Oxidative	BVE	BVE-O-1	229	290	385	0.1
		BVE-O-2	257	316	389	0.2
	BVEL	BVEL-O-1	239	308	394	1.2
		BVEL-O-2	266	326	392	0.2
Inert	BVE	BVE-I	247	313	393	5.7
	BVEL	BVEL-I	239	300	393	5.1

3.5. Tensile Behavior

Figure 6 presents the axial stress vs. axial strain curves obtained in the tensile tests of BVE (Figure 6a) and BVEL resins (Figure 6b). The resins presented a similar behavior up to failure, characterized by an initial linear response, a gradual stiffness reduction before attaining the maximum stress and failing in a brittle manner. Table 6 summarizes the tensile strength, tensile modulus (calculated for strains between 0.1% and 0.5%, for which the response was linear), and the ultimate tensile strain of both types of resins. As shown, BVE and BVEL resins presented similar tensile moduli (3.2–3.4 GPa), yet the incorporation of 4% by the weight of lignin resulted in a 27% increase in tensile strength, and 45% increase in average ultimate tensile strain, which offers a significant advantage for incorporation in FRP composites. This increase in mechanical properties is consistent with the results of GPC tests, namely with the increase in M_w with lignin incorporation. Performance increases have also been reported in previous studies using lignin as a source of hydroxyl groups in polyurethane synthesis, i.e., where lignin acts as a reactive component and is integrated into the polymer structure [49,50]. On the other hand, performance reductions have also been reported in the literature, particularly when lignin is found to behave as a filler [51,52].

It is worth noting that, as shown in Figure 6b, the properties of the BVEL resin showed a slightly higher scatter than those obtained for the BVE resin, possibly owing to the heterogeneity introduced in the main polymeric chains of the former resin via the complex structure of lignin, during the first stage of the polycondensation reaction. This higher heterogeneity has been consistently suggested from the results of the different experiments presented here.

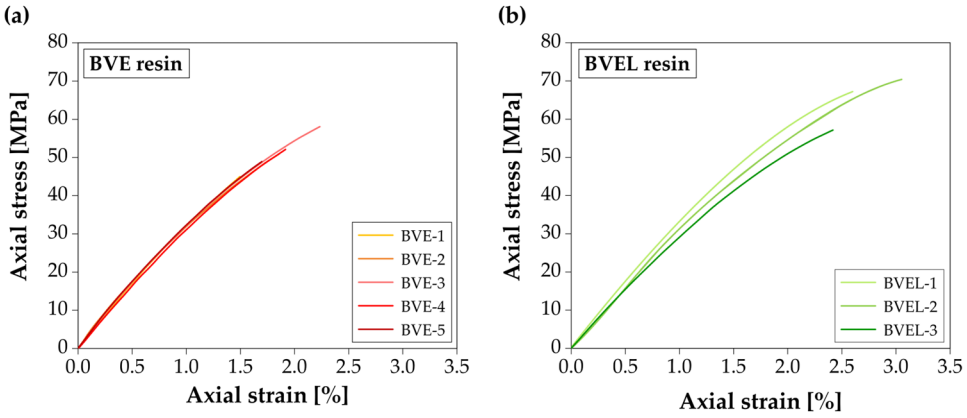

Figure 6. Tensile test results: axial stress vs. axial strain curves obtained for (**a**) BVE and (**b**) BVEL resins.

Table 6. Tensile test results (average ± standard deviation and coefficient of variation (CoV)).

Resin	Specimen	Tensile Strength (MPa)	Tensile Modulus (GPa)	Ultimate Strain (%)
BVE	1	45.0	3.40	1.49
	2	50.9	3.31	1.86
	3	57.9	3.39	2.21
	4	52.1	3.25	1.92
	5	48.9	3.44	1.70
	Average	51.0 ± 4.7 (CoV = 9%)	3.36 ± 0.08 (CoV = 2%)	1.84 ± 0.27 (CoV = 15%)
BVEL	1	67.4	3.43	2.56
	2	70.4	3.18	3.05
	3	57.2	3.08	2.41
	Average	65.0 ± 6.9 (CoV = 11%)	3.23 ± 0.18 (CoV = 6%)	2.67 ± 0.33 (CoV = 13%)

3.6. Shear Behavior

Figure 7 shows the shear stress vs. distortion curves of the BVE (Figure 7a) and BVEL resins (Figure 7b), which showed an initial approximately linear behavior, followed by a non-linear response up to failure characterized by a stiffness reduction with increasing shear stress, typical of polymeric resins; however, this nonlinearity was less pronounced in some of the BVEL specimens, once more being indicative of potentially increased heterogeneity in the polymer structure of this resin. Table 7 summarizes the shear strength, shear modulus (calculated for shear strains between 0.25% and 0.65%, as per ASTM D5379/D5379M) and the ultimate distortion of both resins. The results show that the addition of lignin led to an increase in the average values of the shear properties of the bio-based resin: 4% for shear strength, 11% for shear modulus, and 4% for ultimate distortion. These improvements are consistent with those obtained in the tensile tests, and overall should stem from the same reasons mentioned there.

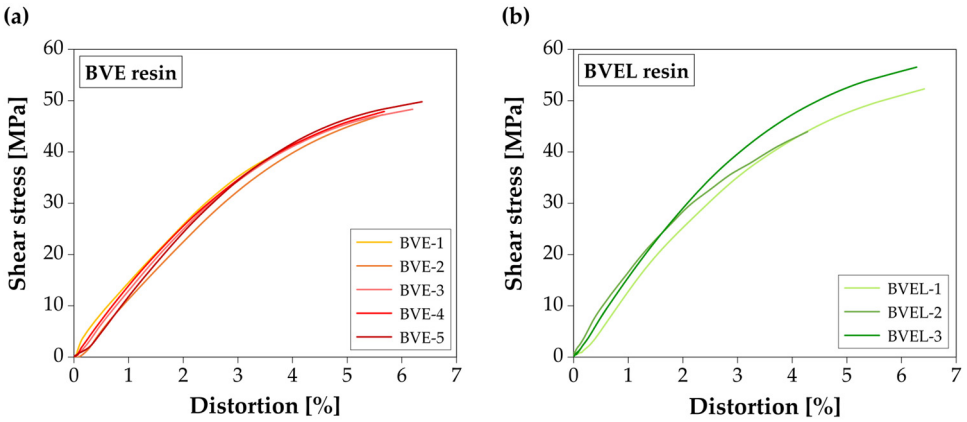

Figure 7. Shear test results: shear stress vs. distortion curves obtained for (**a**) BVE and (**b**) BVEL resins.

Table 7. Shear test results (average ± standard deviation and coefficient of variation (CoV)).

Resin	Specimen	Shear Strength (MPa)	Shear Modulus (GPa)	Ultimate Distortion (%)
BVE	1	49.6	1.37	4.31
	2	47.2	1.51	5.65
	3	48.2	1.57	6.19
	4	47.8	1.45	5.67
	5	57.4	1.67	6.61
	Average	50.0 ± 4.2 (CoV = 8%)	1.51 ± 0.11 (CoV = 8%)	5.69 ± 0.87 (CoV = 15%)
BVEL	1	52.1	1.51	6.41
	2	47.5	1.68	5.02
	3	56.3	1.86	6.27
	Average	52.0 ± 4.4 (CoV = 8%)	1.68 ± 0.18 (CoV = 10%)	5.90 ± 0.77 (CoV = 13%)

4. Conclusions

This paper investigated the effects of the incorporation of Kraft lignin obtained through the Lignoboost process from Eucalyptus wood on a partially bio-based vinyl ester (VE) resin. The study focused on the impacts of such an incorporation on the short-term mechanical properties (tensile and shear) and thermomechanical properties (i.e., glass transition and decomposition temperatures) of the base resin.

The incorporation of 4% wt. of lignin resulted in a more amorphous (less crystalline) and heterogenous polymer chain with reduced mobility due to lignin's relatively complex and high molecular weight aromatic structure. In practical terms, this was reflected in the improvement of the mechanical and thermomechanical properties of the base resin: the tensile strength increased 27% and the shear strength increased 4%; an improvement was also observed for the glass transition temperature (defined based on the tan δ peak), which increased from the 95–98 °C range to the 102–107 °C range. The VE resin with lignin incorporation also evidenced significant potential for additional cross-linking, even after a post-cure of 4 h at 100 °C. On the other hand, the resin with lignin incorporation showed a somewhat increased scatter in its mechanical response, particularly at higher stress levels, as well as higher brittleness. The tensile and shear moduli and the decomposition temperature were fairly similar to those of the reference resin without lignin.

Overall, these results demonstrate that, despite requiring curing at high temperature, a minor incorporation of lignin can significantly improve the thermomechanical and mechanical behavior of bio-based VE resin. These results seem to confirm the promising potential of

using this sustainable biopolymer in high-performance composite applications. However, the further assessment of the influence of lignin incorporation fraction on the properties of the resulting resins as well as their compatibility with typical fiber reinforcements are still necessary.

Author Contributions: Conceptualization. J.C.B., M.M. and M.H.; methodology. J.C.B., M.H., M.M. and M.G.; investigation. M.M., M.H., M.G., J.R.C., J.C.B. and I.C.R.; resources. J.R.C. and M.G.; data curation. M.M.; writing—original draft preparation. I.C.R. and M.M.; writing—review and editing. I.C.R., M.M., M.H., M.G., J.C.B. and J.R.C.; visualization. M.M. and I.C.R.; supervision. M.G., J.R.C. and J.C.B.; project administration. M.G. and J.R.C.; funding acquisition. M.G. and J.R.C. All authors have read and agreed to the published version of the manuscript.

Funding: This research was funded by the Portuguese National Innovation Agency (ANI) and Portuguese Foundation for Science and Technology (FCT) through projects *BioLam* (POCI-01-0247-FEDER-039769-LISBOA 01-0247-FEDER-039769) and *EcoComposite* (PTDC/ECI-EGC/29597/2017), respectively. This work is also part of the research activity carried out at the Civil Engineering Research and Innovation for Sustainability (CERIS) research unit and was funded by the FCT in the framework of project UIDB/04625/2020. The first author also wishes to thank the FCT for their financial support through the scholarship SFRH/BD/04675/2020.

Institutional Review Board Statement: Not applicable.

Informed Consent Statement: Not applicable.

Data Availability Statement: The data presented in this study are available on request from the corresponding author.

Conflicts of Interest: The authors declare no conflict of interest.

References

1. Lima, L.; Trindade, E.; Alencar, L.; Alencar, M.; Silva, L. Sustainability in the construction industry: A systematic review of the literature. *J. Clean. Prod.* **2020**, *289*, 125730. [CrossRef]
2. Construction Leadership Council. The Routemap for Zero Avoidable Waste in Construction. 2021. Available online: https://www.constructionleadershipcouncil.co.uk/wp-content/uploads/2021/07/ZAW-Interactive-Routemap-FINAL.pdf (accessed on 1 June 2023).
3. Sonmez, F.O. Optimum Design of Composite Structures: A Literature Survey (1969–2009). *J. Reinf. Plast. Compos.* **2016**, *36*, 3–39. [CrossRef]
4. Aggarwal-Khan, S. *How Can a Life-Cycle Approach Curb the Plastic Pollution Crisis*; UNEP United Nations Environment Programme: Nairobi, Kenya, 2022; Available online: https://policycommons.net/artifacts/2618339/how-can-a-life-cycle-approach-curb-the-plastic-pollution-crisis/3640927 (accessed on 1 June 2023).
5. Hofmann, M.A.; Shahid, A.T.; Garrido, M.; Ferreira, M.J.; Correia, J.R.; Bordado, J.C. Biobased Thermosetting Polyester Resin for High-Performance Applications. *ACS Sustain. Chem. Eng.* **2022**, *10*, 3442–3454. [CrossRef]
6. Hofmann, M.; Garrido, M.; Machado, M.; Correia, J.R.; Bordado, J.C. Development of high-performance partially biobased thermoset polyester using renewable building blocks from isosorbide, 1,3-propanediol, and fumaric acid. *J. Appl. Polym. Sci.* **2022**, *139*, e53029. [CrossRef]
7. Alzagameem, A.; El Khaldi-Hansen, B.; Kamm, B.; Schulze, M. Lignocellulosic biomass for energy, biofuels, biomaterials and chemicals. In *Biomass and Green Chemistry*; Sílvio, V., Jr., Ed.; Springer: Cham, Switzerland, 2018.
8. Collins, M.N.; Nechifor, M.; Tanasă, F.; Zănoagă, M.; McLoughlin, A.; Stróżyk, M.A.; Culebras, M.; Teacă, C.-A. Valorization of lignin in polymer and composite systems for advanced engineering applications—A review. *Int. J. Biol. Macromol.* **2019**, *131*, 828–849. [CrossRef] [PubMed]
9. Asim, M.; Saba, N.; Jawaid, M.; Nasir, M.; Pervaiz, M.; Alothman, O.Y. A review on phenolic resin and its composites. *Curr. Anal. Chem.* **2017**, *13*, 185–197. [CrossRef]
10. Pan, H. Synthesis of polymers from organic solvent liquefied biomass: A review. *Renew. Sustain. Energy Rev.* **2011**, *15*, 3454–3463. [CrossRef]
11. Kun, D.; Pukánszky, B. Polymer/lignin blends: Interactions, properties, applications. *Eur. Polym. J.* **2017**, *93*, 618–641. [CrossRef]
12. Bakis, C.E.; Bank, L.C.; Brown, V.L.; Cosenza, E.; Davalos, J.F.; Lesko, J.J.; Machida, A.; Rizkalla, S.H.; Triantafillou, T.C. Fiber-Reinforced Polymer Composites for Construction—State-of-the-Art Review. *J. Compos. Constr.* **2002**, *6*, 73–87. [CrossRef]
13. Davis, K.M.; Rover, M.; Brown, R.C.; Bai, X.; Wen, Z.; Jarboe, L.R. Recovery and Utilization of Lignin Monomers as Part of the Biorefinery Approach. *Energies* **2016**, *9*, 808. [CrossRef]

14. Frollini, E.; Silva, C.; Ramires, E. Phenolic resins as a matrix material in advanced fiber-reinforced polymer (FRP) composites. In *Advanced Fibre-Reinforced Polymer (FRP) Composites for Structural Applications*; Bai, J., Ed.; Woodhead Publishing Series in Civil and Structural Engineering: Sawston, UK, 2013; pp. 7–43. [CrossRef]
15. Trinowski, D.M. Foundry. In *Phenolic Resins: A Century of Progress*; Louis, P., Ed.; Springer: Berlin/Heidelberg, Germany, 2010; pp. 451–502.
16. dos Santos, R.G.; Acero, N.F.; Matos, S.; Carvalho, R.; Vale, M.; Marques, A.C.; Bordado, J.C.; Mateus, M.M. One-Component Spray Polyurethane Foam from Liquefied Pinewood Polyols: Pursuing Eco-Friendly Materials. *J. Polym. Environ.* **2017**, *26*, 91–100. [CrossRef]
17. dos Santos, R.G.; Carvalho, R.; Silva, E.R.; Bordado, J.C.; Cardoso, A.C.; Costa, M.D.R.; Mateus, M.M. Natural polymeric water-based adhesive from cork liquefaction. *Ind. Crop. Prod.* **2016**, *84*, 314–319. [CrossRef]
18. Domínguez, J.C.; Oliet, M.; Alonso, M.V.; Rojo, E.; Rodríguez, F. Structural, thermal and rheological behavior of a bio-based phenolic resin in relation to a commercial resol resin. *Ind. Crops Prod.* **2013**, *42*, 308–314. [CrossRef]
19. van Haveren, J.; Oostveen, E.A.; Micciché, F.; Noordover, B.A.J.; Koning, C.E.; van Benthem, R.A.T.M.; Frissen, A.E.; Weijnen, J.G.J. Resins and additives for powder coatings and alkyd paints, based on renewable resources. *J. Coat. Technol. Res.* **2007**, *4*, 177–186. [CrossRef]
20. Solt, P.; Rößiger, B.; Konnerth, J.; Van Herwijnen, H.W.G. Lignin Phenol Formaldehyde Resoles Using Base-Catalysed Depolymerized Kraft Lignin. *Polymers* **2018**, *10*, 1162. [CrossRef]
21. Zhang, Y.; Li, N.; Chen, Z.; Ding, C.; Zheng, Q.; Xu, J.; Meng, Q. Synthesis of High-Water-Resistance Lignin-Phenol Resin Adhesive with Furfural as a Crosslinking Agent. *Polymers* **2020**, *12*, 2805. [CrossRef]
22. Galdino, D.S.; Kondo, M.Y.; De Araujo, V.A.; Ferrufino, G.L.A.A.; Faustino, E.; dos Santos, H.F.; Christoforo, A.L.; Luna, C.M.R.; de Campos, C.I. Thermal and Gluing Properties of Phenol-Based Resin with Lignin for Potential Application in Structural Composites. *Polymers* **2023**, *15*, 357. [CrossRef]
23. Aristri, M.A.; Lubis, M.A.R.; Yadav, S.M.; Antov, P.; Papadopoulos, A.N.; Pizzi, A.; Fatriasari, W.; Ismayati, M.; Iswanto, A.H. Recent Developments in Lignin- and Tannin-Based Non-Isocyanate Polyurethane Resins for Wood Adhesives—A Review. *Appl. Sci.* **2021**, *11*, 4242. [CrossRef]
24. Guigo, N.; Mija, A.; Vincent, L.; Sbirrazzuoli, N. Eco-friendly composite resins based on renewable biomass resources: Polyfurfuryl alcohol/lignin thermosets. *Eur. Polym. J.* **2010**, *46*, 1016–1023. [CrossRef]
25. Asada, C.; Basnet, S.; Otsuka, M.; Sasaki, C.; Nakamura, Y. Epoxy resin synthesis using low mo-lecular weight lignin separated from various lignocellulosic materials. *Int. J. Biol. Macromol.* **2015**, *74*, 413–419. [CrossRef]
26. Li, R.J.; Gutierrez, J.; Chung, Y.-L.; Frank, C.W.; Billington, S.L.; Sattely, E.S. A lignin-epoxy resin derived from biomass as an alternative to formaldehyde-based wood adhesives. *Green Chem.* **2018**, *20*, 1459–1466. [CrossRef]
27. Li, W.X.; Xiao, L.P.; Li, X.Y.; Xiao, W.Z.; Yang, Y.Q.; Sun, R.C. Renewable and flexible thermosetting epoxies based on functionalized biorefinery lignin fractions. *Mater. Today Sustain.* **2021**, *15*, 100083. [CrossRef]
28. Kai, D.; Zhang, K.; Jiang, L.; Wong, H.Z.; Li, Z.; Zhang, Z.; Loh, X.J. Sustainable and Antioxidant Lignin–Polyester Copolymers and Nanofibers for Potential Healthcare Applications. *ACS Sustain. Chem. Eng.* **2017**, *5*, 6016–6025. [CrossRef]
29. Wang, X.; Jia, Y.; Liu, Z.; Miao, J. Influence of the Lignin Content on the Properties of Poly(Lactic Acid)/lignin-Containing Cellulose Nanofibrils Composite Films. *Polymers* **2018**, *10*, 1013. [CrossRef]
30. Pączkowski, P.; Puszka, A.; Gawdzik, B. Investigation of Degradation of Composites Based on Unsaturated Polyester Resin and Vinyl Ester Resin. *Materials* **2022**, *15*, 1286. [CrossRef]
31. Rogers, D. Lignin-Derived Thermosetting Vinyl Ester Resins for High Performance Applications. Master's Thesis, Rowan University, Glassboro, NJ, USA, 2015.
32. Podkościelna, B.; Wnuczek, K.; Goliszek, M.; Klepka, T.; Dziuba, K. Flammability Tests and Investigations of Properties of Lignin-Containing Polymer Composites Based on Acrylates. *Molecules* **2020**, *25*, 5947. [CrossRef]
33. Goliszek, M.; Podkościelna, B.; Klepka, T.; Sevastyanova, O. Preparation, Thermal, and Mechanical Characterization of UV-Cured Polymer Biocomposites with Lignin. *Polymers* **2020**, *12*, 1159. [CrossRef]
34. Pilato, L. Phenolic resins: 100Years and still going strong. *React. Funct. Polym.* **2013**, *73*, 270–277. [CrossRef]
35. Tang, K.; Zhang, A.; Ge, T.; Liu, X.; Tang, X.; Li, Y. Research progress on modification of phenolic resin. *Mater. Today Commun.* **2020**, *26*, 101879. [CrossRef]
36. Gardziella, A.; Pilato, L.A.; Knop, A. *Phenolic Resins—Chemistry, Applications, Standardization, Safety and Technology*; Springer: Berlin/Heidelberg, Germany, 2000.
37. Pilato, L. Future Aspects. In *Phenolic Resins: A Century of Progress*; Springer: Berlin/Heidelberg, Germany, 2010.
38. Notley, S.M.; Norgren, M. Lignin: Functional biomaterial with potential in surface chemistry and nanoscience. In *The Nanoscience and Technology of Renewable Biomaterials*; Lucia, L.A., Rojas, O.J., Eds.; Wiley-Blackwell: Hoboken, NJ, USA, 2009; pp. 173–205.
39. Noh, Y.; Odimayomi, T.; Sendesi, S.M.T.; Youngblood, J.P.; Whelton, A.J. Environmental and human health risks of plastic composites can be reduced by optimizing manufacturing conditions. *J. Clean. Prod.* **2022**, *356*, 131803. [CrossRef]
40. *ASTM E1640-09*; Standard Test Method for Assignment of the Glass Transition Temperature by Dynamic Mechanical Analysis. American Society for Testing and Materials: West Conshohocken, PA, USA, 2009.
41. *ASTM E2550-21*; Standard Test Method for Thermal Stability by Thermogravimetry. American Society for Testing and Materials: West Conshohocken, PA, USA, 2021.

42. *ASTM D638-14*; Standard Test Method for Tensile Properties of Plastics. American Society for Testing and Materials: West Conshohocken, PA, USA, 2014.
43. *ASTM D5379/D5379M-12*; Standard Test Method for Shear Properties of Composite Materials by the V-Notched Beam Method. American Society for Testing and Materials: West Conshohocken, PA, USA, 2010.
44. Costa, C.S.M.F.; Fonseca, A.C.; Moniz, J.; Godinho, M.; Coelho, J.; Serra, A.C. Going greener: Synthesis of fully biobased unsaturated polyesters for styrene crosslinked resins with enhanced thermomechanical properties. *Express Polym. Lett.* **2017**, *11*, 885–898. [CrossRef]
45. Ferreira, G.R.; Braquehais, J.R.; da Silva, W.N.; Machado, F. Synthesis of soybean oil-based polymer lattices via emulsion polymerization process. *Ind. Crop. Prod.* **2015**, *65*, 14–20. [CrossRef]
46. Papadopoulos, L.; Malletzidou, L.; Patsiaoura, D.; Magaziotis, A.; Psochia, E.; Terzopoulou, Z.; Chrissafis, K.; Markessini, C.; Papadopoulou, E.; Bikiaris, D.N. Synthesis and Characterization of Unsaturated Succinic Acid Biobased Polyester Resins. *Appl. Sci.* **2021**, *11*, 896. [CrossRef]
47. Kang, H.; Li, M.; Tang, Z.; Xue, J.; Hu, X.; Zhang, L.; Guo, B. Synthesis and characterization of biobased isosorbide-containing copolyesters as shape memory polymers for biomedical applications. *J. Mater. Chem. B* **2014**, *2*, 7877–7886. [CrossRef]
48. Trino, A.; Costa, C.; Fonseca, A.; Barata, I.; Júlio, E.; Serra, A.; Coelho, J. Novel composites from green unsaturated polyesters and fly ashes: Preparation and characterization. *React. Funct. Polym.* **2016**, *106*, 24–31. [CrossRef]
49. Xue, B.-L.; Wen, J.-L.; Zhu, M.-Q.; Sun, R.-C. Lignin-based polyurethane film reinforced with cellulose nanocrystals. *RSC Adv.* **2014**, *4*, 36089–36096. [CrossRef]
50. Jia, Z.; Lu, C.; Zhou, P.; Wang, L. Preparation and characterization of high boiling solvent lignin-based polyurethane film with lignin as the only hydroxyl group provider. *RSC Adv.* **2015**, *5*, 53949–53955. [CrossRef]
51. Sarkar, S.; Adhikari, B. Synthesis and characterization of lignin–HTPB copolyurethane. *Eur. Polym. J.* **2001**, *37*, 1391–1401. [CrossRef]
52. Jeong, H.; Park, J.; Kim, S.; Lee, J.; Cho, J.W. Use of acetylated softwood kraft lignin as filler in synthetic polymers. *Fibers Polym.* **2012**, *13*, 1310–1318. [CrossRef]